J Fluoresc (2011) 21:497–506
DOI 10.1007/s10895-010-0736-8

ORIGINAL PAPER

A Series of Carbazole Cationic Compounds with Large Two-Photon Absorption Cross Sections for Imaging Mitochondria in Living Cells with Two-Photon Fluorescence Microscopy

Xin Liu · Yuming Sun · Yuanhong Zhang · Ning Zhao · Hongshi Zhao · Guancong Wang · Xiaoqiang Yu · Hong Liu

Received: 5 July 2010 / Accepted: 28 September 2010 / Published online: 16 October 2010

Abstract A series of carbazole cationic compounds based on donor- Π—acceptor (D-Π-A) structure were synthesized and characterized. They exhibit large two-photon absorption cross sections when excited by a 810 nm a laser beam, and their photophysical properties show that the intramolecular charge transfer (ICT) character is predominant. Moreover these compounds can easily pass though the intact cell membrane of living cells, amongst, 3-(1-hydroxyethyl -4-vinylpyridium iodine)-N-butyl carbazole (9B-HVC) has been proven to be capable of accumulating within the mitochondria possessing large membrane potential and imaging this organelle in living cells by means of two-photon fluorescence microscopy. At the same time usable fluorescent photos can be obtained at lower incident excitation power (5 mW) and low-micromolar concentrations (2 μM), which does not result in significant reduction in cell viability over a period of at least 24 h.

Keywords Two-photon microscopy · Mitochondria · Fluorescent probe · Living cells

X. Liu · Y. Zhang · N. Zhao · H. Zhao · G. Wang · X. Yu (✉) · H. Liu (✉)
State Key Laboratory of Crystal Materials, Shandong University, Jinan 250100, People's Republic of China
e-mail: yuxq@sdu.edu.cn

H. Liu
e-mail: hongliu@sdu.edu.cn

Y. Sun
Optics Department, Shandong University, Jinan 250100, People's Republic of China

Introduction

Extensive biochemical studies on mitochondria have proved that they play a cardinal role on cell function and dysfunction. Mitochondria not only contribute to the generation of energy essential for the survival and proliferation of eukaryotic cells, but also implicate in the regulation of programmed cell death, reactive oxygen species generation, and maintenance of calcium homeostasis [1–4]. In particular, mitochondria show remarkable plasticity, mobility, and morphological heterogeneity occurring in conjunction with the metabolic state of the cell, cell cycle, cellular development and differentiation, and pathological states [5–7]. Therefore, many approaches have been adopted to study the structure and function of mitochondria.

Fluorescence imaging technique with application of fluorescent probes allowing high-resolution visualization of different organelles has been considered as the valid method and used in various studies of mitochondria [8, 9]. Currently, two-photon fluorescence microscopy (TPM), a revolutionary development of fluorescence imaging technique, exhibits many unique capabilities in imaging of living specimens. Adopting two-photon absorption mechanism, TPM utilize the long wavelength incident beam in IR region as exciting source thus avoiding the photodamage of UV-vis to living specimen [10, 11]. Recently, by using TPM, many important biological works relevant to study of life phenomenon have been accomplished [12–16], including those involved to mitochondria [17, 18]. However, both of theoretical prediction and practical work have indicated that the superiority of TPM have been hampered due to using the conventional fluorescent probes with small two-photon absorption cross sections (δ_{TPA}), which demanded

impractically high laser power [10, 19]. When these probes are used on TPM, only a little portion of the large excitation power could be utilized to generate fluorescence, and the rest would cause heatdamage to the living specimen and high-order photobleaching of substrate [20, 21]. Accordingly, design and synthesis of two-photon induced fluorescence (TPF) probes with large δ_{TPA} have been being desired and some excellent results on this work have been reported [22–25]. To our best knowledge, TPF probes targeting to mitochondria are seldom reported. Therefore, it is significant yet practically needed to develop efficient TPF mitochondria probes with large δ_{TPA}, which will improve the further study of the complex organelles.

Until now, many mitochondria-targeted antioxidants, anticancer drugs and fluorescent probes of mitochondria have been exploited in response to the large mitochondrial membrane potential [26–28]. These molecules commonly are the lipophilic cationic compounds with the large ionic radius which is inversely proportional to the enthalpy required to move the cationics through the hydrophobic core of the membrane [29, 30]. Upon this point, we design and synthesize a series D-π-A type carbazole cationics to explore the TPF mitochondria probes (Scheme 1). As well known, carbazole has been shown to be promising substrates for two-photon absorption (TPA) applications due to their rigid plane and long conjugation length [31]. In this paper, the carbazole cationic compounds, 3-(1-methyl-4-vinylpyridium iodine) carbazole (MVC), 3-(1-hydroxyethyl-4-vinylpyridium iodine)carbazole (HVC), 3-(1-methyl-4-vinylpyridium iodine)-N-butyl carbazole (9B-MVC) and 3-(1- hydroxyethyl -4-vinylpyridium iodine)-N-butyl carbazole (9B-HVC), were synthesized. In these compounds, carbazole was introduced to probe molecules as the donor, and the molecular pi-electron conjugated system was enlarged by forming—CH=CH– in 3-position of carbazole. The cationic pyridinium unit as acceptor groups was bound on other side of vinyl bond [32]. Compared to MVC and HVC, the introduction of a butyl group in place of a H atom at 9-position of carbazole in 9B-MVC and 9B-HVC is to enhance the electron-donating ability of carbazole, and a hydroxylethyl in HVC and 9B-HVC in the place of the methyl in MVC and 9B-MVC to quaternize the *N*-pyridinium atom is for better hydrophilicity. In these structures, the cationic pyridinium can offer net positive charge for the molecular, and the large conjugate system which is composed of carbazole, vinyl and cationic pyridinium ensures the large ionic radius. Excitedly, these compounds not only exhibit the large δ_{TPA}, but also 9B-HVC can exclusively label mitochondria.

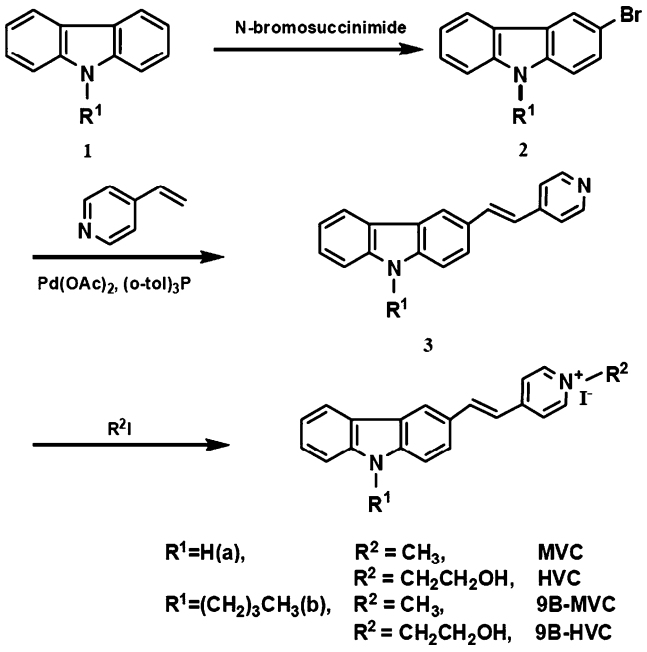

Scheme 1 Synthetic route of MVC, HVC, 9B-MVC and 9B-HVC

Furthermore, their single- and two-photon spectroscopic properties in various environments were investigated to elucidate the luminescence mechanism systematically. The imaging application of 9B-HVC for mitochondria was carefully evaluated with wide-field fluorescence microscopy (WFM) and TPM. In addition, the cytotoxicity was also analyzed for choosing the suitable staining conditions.

Experimental

Synthesis

N-Butylcarbazole(1b) 13.2 g (80 mmol) of carbazole were added into the solution of 28 g (500 mmol) KOH in 60 mL acetone at the conditions of stirring and room temperature. After 4 h, a solution of 1-bromobutane (13 mL, 120 mmol) in acetone was added to the mixture above and then maintained 24 h. The final solution was poured into 1 L water and yellow suspended matter was obtained. The products were filtrated and recrystallized in ethanol. White solid were obtained, yield: 81%.^{1}H NMR (300 MHz, $CDCl_3$) δ(ppm): 8.10 (d, *J*=7.8 Hz, 2 H), 7.44(m, 4 H), 7.22(m, 2 H), 4.3(t, *J*=7.2 Hz, 2 H), 1.80–1.90 (m, 2 H), 1.34–1.46 (m, 2 H), 0.94 (t, *J*=7.4 Hz, 3 H).

3-Bromocarbazole(2a)/3-bromo-N-butylcarbazole(2b) To the CH2Cl2 solution of 3.56 g (20 mmol) *N*-bromosuccinimide (NBS) was added the of carbazole (3.34 g, 20 mmol) or *N*-butylcarbazole (4.46 g, 20 mmol) dissolved in CH2Cl2/acetone mixture solution, and the resulting solution was stirred at room temperature for 24 h. The mixture was washed several times with water and saturated NaCl solution, the organic phases was separated and the excess organic solvent was removed by vacuum distillation. The residue was purified by column chromatography with ethyl-

acetate/petroleum ether (10:1) as eluent, finally the white solid was obtained for 3-bromocarbazole, yield: 62%. ^{1}H NMR (300 MHz, DMSO) δ(ppm):11.4(s, 1H), 8.35(d, *J*= 1.8 Hz, 1H), 8.17(d, *J*=7.8 Hz, 1H), 7.39–7.51 (m, 4 H), 7.15–7.20 (m, 1H). White yellow oil was obtained for 3-bromo-*N*-butylcarbazole, yield: 53%. ^{1}H NMR (400 MHz, DMSO) δ(ppm): 8.41(d, *J*=1.8 Hz, 1H), 8.20(d, *J*=7.8 Hz, 1H), 7.45–7.60(m, 4 H), 7.23(t, *J*=7.7 Hz, 1H), 4.30(t, *J*= 7.0 Hz, 2 H), 1.64–1.71(m, 2 H), 1.18–1.27(m, 2 H), 0.81(t, *J*=7.3 Hz, 3 H).

3-(4-Vinylpyridium)Carbazole(3a) The 3-bromo-carbazole (0.50 g, 2 mmol) was added into a high pressure bottle containing the mixture of Palladium(II) acetate (4.0 mg, 0.02 mmol) and tri-*o*-tolyl phosphine (40.0 mg, 0.13 mmol), then to which was added the solvent pair (triethylamine 6 mL/tetrahydrofuran 18 mL) and 4-vinylpyridine (0.42 g, 4 mmol). The bottle was sealed after bubbling 10 min with nitrogen. After keeping the system under ~100 °C for three days, the mixture was poured into water and orange solid was obtained. After filtration, the precipitate was purified by column chromatography with ethyl-acetate/ petroleum ether (1:2) as eluent, and the yellow solid was obtained, yield: 35%.^{1}H NMR (400 MHz, DMSO-d_6) δ(ppm): 11.42 (s, 1H), 8.53(d, *J*=5.9 Hz, 2 H), 8.43 (s, 1H), 8.15(d, *J*=7.7 Hz, 1H), 7.69–7.75 (m, 2 H), 7.56(d, *J*=6.0 Hz, 2 H), 7.50–7.52(m, 2 H), 7.40–7.43(m, 1H), 7.18–7.26(m, 2 H).

3-(4-Vinylpyridium)-N-Butylcarbazole(3b) 2.0 g (6.0 mmol) of 3-bromo-*N*-butyl-carbazole was added into a flask containing mixture of palladium(II) acetate (0.13 g, 0.6 mmol), tri-o-tolylphosphine (0.54 g, 1.8 mmol) and K_2CO_3(4.1 g, 30.0 mmol), then to which was added the solvent NMP (50 mL) and 4-vinylpyridine (1.68 g, 16.0 mmol). Under the protection of argon, the system was heated at 130 °C for 2 days and dark-red suspending solution was obtained. After pouring the reaction solution to 1 L H_2O, the mixture was extracted by ethyl acetate. The organic phase was separated and the excess organic solvent was removed by vacuum distillation and dark-red solution was obtained. The solution was purified by column chromatography with ethyl-acetate/petroleum ether (1:2) as eluent, and the titled product was obtained as yellow solid. Yield: 60%. ^{1}H NMR (400 MHz, DMSO-d_6) δ(ppm): 8.54(d, *J*=6.0 Hz, 2 H), 8.46 (d, *J*=0.9 Hz, 1H), 8.19(d, *J*= 7.7 Hz, 1H), 7.78–7.80(m, 1H), 7.72(d, *J*=16.4 Hz, 1H), 7.63(t, *J*=8.4 Hz, 2 H), 7.57(d, *J*=6.0 Hz, 2 H), 7.46–7.50 (m, 1H), 7.22–7.28(m, 2 H), 4.41(t, *J*=7.0 Hz, 2 H), 1.73–1.78(m, 2 H), 1.28–1.34(m, 2 H), 0.89(t, *J*=7.4 Hz, 3 H).

3-(1-Methyl-4-Vinylpyridium iodine)Carbazole(MVC), 3-(1-Hydroxyethyl-4-Vinylpyridium iodine)Carbazole(HVC), 3-(1-Methyl-4-Vinylpyridium Iodine)-N-Butyl Carbazole(9B-MVC) and 3-(1- Hydroxyethyl -4-Vinylpyridium Iodine)-N-Butyl Carbazole(9B-HVC) After refluxing the *3-(4-vinylpyridium)carbazole/3-(4-vinylpyridium)-N-butylcarbazole* with excess ICH_3/ICH_2CH_2OH in acetone for overnight, the crude product was collected as powder. After recrystalization from methanol, title products were obtained. For MVC, yellow solid, yield: 85%, ^{1}H NMR (400 MHz, DMSO-d_6) δ(ppm): 11.65 (s, 1H), 8.80(d, *J*=6.8 Hz, 2 H), 8.56 (s, 1H), 8.16–8.23(m, 4 H), 7.83–7.85(m, 1H), 7.43–7.60 (m, 4H), 7.23–7.27 (m, 1H), 4.23(s, 3H). ^{13}C NMR (100 MHz, DMSO-d_6): δ 153.6, 145.2, 143.0, 141.7, 140.8, 126.8, 126.6, 126.5, 123.5, 123.2, 122.8, 121.7, 120.8, 120.2, 120.0, 112.1, 112.0, 47.1. HRMS (m/z): $[M-I]^+$ calcd for $C_{20}H_{17}N_2I$, 285.36; found, 285.2. Elemental analysis calcd (%) for $C_{20}H_{17}N_2I$ (412.27): C 58.27, H 4.16, N 6.79; found: C 58.07, H 4.26, N 6.93.

For HVC, red solid, yield: 78%, ^{1}H NMR (400 MHz, DMSO-d_6) δ(ppm): 11.65 (s, 1H), 8.82(d, *J*=6.8 Hz, 2 H), 8.57 (s, 1H), 8.16–8.24(m, 4H), 7.83–7.86(m, 1H), 7.43–7.60(m, 4 H), 7.25(t, *J*=7.4 Hz, 1H), 5.26(s, 1H), 4.54(t, *J*=4.7 Hz, 2 H), 3.87(s, 2 H). ^{13}C NMR (100 MHz, DMSO-d_6): δ 154.1, 144.8, 143.2, 141.7, 140.8, 126.8, 126.7, 126.5, 123.5, 123.2, 122.8, 121.7, 120.8, 120.2, 120.0, 112.1, 112.0, 62.3, 60.5. HRMS (m/z): $[M-I]^+$ calcd for $C_{21}H_{19}N_2IO$, 315.39; found, 315.2. Elemental analysis calcd (%) for $C_{21}H_{19}N_2IO$ (442.29): C 57.03, H 4.33, N 6.33; found: C 56.92, H 4.39, N 6.47.

For 9B-MVC, yellow solid, yield: 89%, ^{1}H NMR (400 MHz, DMSO-d_6) δ(ppm): 8.80(d, *J*=6.8 Hz, 2 H), 8.60(s, 1H), 8.18–8.23(m, 4 H), 7.88–7.90(m, 1H), 7.74(d, *J*=8.6 Hz, 1H), 7.67(d, *J*=8.2 Hz, 1H), 7.51–7.55(m, 2 H), 7.29(t, *J*=7.4 Hz, 1H), 4.45(t, *J*=7.0 Hz, 2 H), 4.24(s, 3 H), 1.76–1.80(m, 2 H), 1.29–1.35(m, 2 H), 0.89(t, *J*=7.4 Hz, 3 H). ^{13}C NMR (100 MHz, DMSO-d_6): δ 153.5, 145.2, 142.8, 141.9, 141.1, 126.9, 126.7, 126.6, 123.2, 123.1, 122.5, 121.6, 120.9, 120.4, 120.1, 110.6, 110.4, 47.1, 42.7, 31.2, 20.2, 14.2. HRMS (m/z): $[M-I]^+$ calcd for $C_{24}H_{25}N_2I$, 341.47; found, 341.4. Elemental analysis calcd (%) for $C_{24}H_{25}N_2I$ (468.37): C 61.54, H 5.38, N 5.98; found: C 61.76, H 5.39, N 6.17.

For 9B-HVC, yellow solid, yield: 92%, ^{1}H NMR (400 MHz, DMSO-d_6) δ(ppm): 8.82(d, *J*=6.8 Hz, 2 H), 8.59(s, 1H), 8.19–8.24(m, 4H), 7.89–7.91(m, 1H), 7.74(d, *J*=8.6 Hz, 1H), 7.67(d, *J*=8.2 Hz, 1H), 7.50–7.56(m, 2 H), 7.29(t, *J*=7.4 Hz, 1H), 5.24(t, *J*=5.2 Hz, 1H), 4.54(t, *J*= 4.8 Hz, 2H), 4.45(t, *J*=7.0 Hz, 2H), 3.85–3.89(m, 2H), 1.78 (t, *J*=7.5 Hz, 2H), 1.29–1.35(m, 2H), 0.89(t, *J*=7.4 Hz, 3H). ^{13}C NMR (100 MHz, DMSO-d_6): δ 154.0, 144.9, 143.0, 141.9, 141.1, 126.9, 126.8, 126.7, 123.2, 123.1, 122.4, 121.6, 120.9, 120.4, 120.1, 110.6, 110.4, 62.3, 60.5, 42.7, 31.2, 20.2, 14.2. HRMS (m/z): $[M-I]^+$ calcd for $C_{25}H_{27}N_2IO$, 371.49; found, 371.4. Elemental analysis

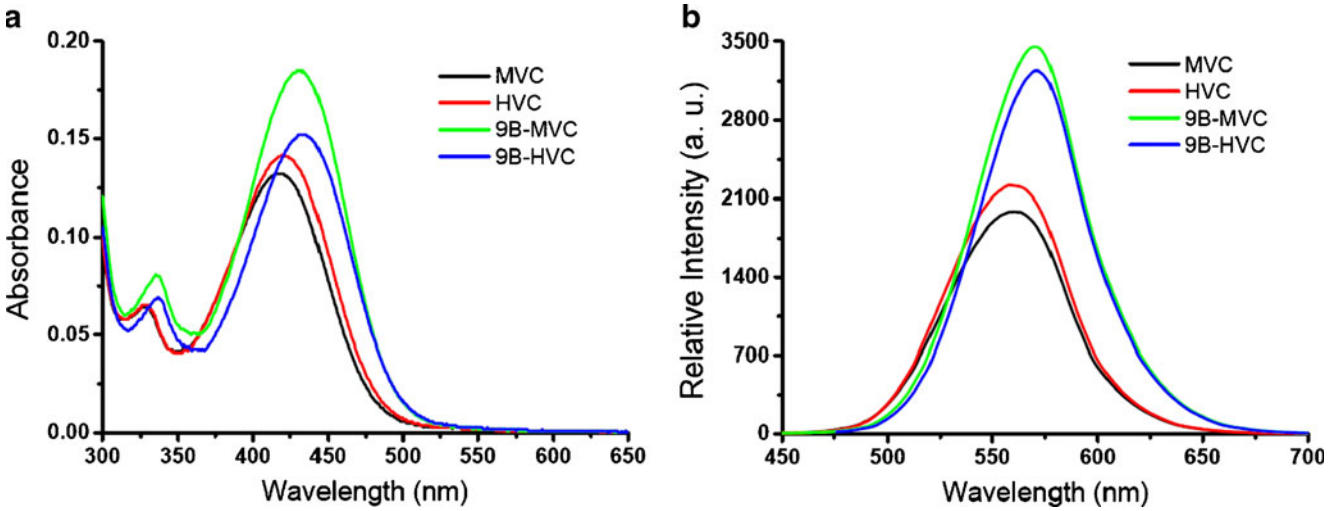

Fig. 1 UV-vis absorption spectra (**a**) and single-photon excited fluorescence spectra (**b**) of four compounds in MeCN at an identical concentration of 5.0×10^{-6} M

calcd (%) for $C_{25}H_{27}N_2IO$(498.40): C 60.25, H 5.46, N 5.62; found: C 60.22, H 5.50, N 5.70.

Instruments and Measurements

The UV-visible-near-IR absorption spectra of dilute solutions were recorded on a UV-2550 spectrophotometer using a quartz cuvette having 1 cm path length. One-photon fluorescence spectra were obtained on a HITACH F-4500 spectrofluorimeter equipped with a 450-W Xe lamp. Two-photon ones were noted on a SpectroPro300i and the pump laser beam come from a mode-locked Ti:sapphire laser system at the pulse duration of 200 fs, with a repetition rate of 76 MHz (Coherent Mira900-D).

TPA cross sections have been measured using the two-photon induced fluorescence method [33, 34], and thus cross sections can be calculated with coumarin 307 in water as reference [34] by means of equation (1)

$$\delta_s = \delta_r \frac{\Phi_r}{\Phi_s}\frac{c_r}{c_s}\frac{n_r}{n_s}\frac{F_s}{F_r} \quad (1)$$

where the subscripts s and r refer to the sample and the reference material, respectively. δ is the TPA cross sectional value, c is the concentration of the solution, n is the refractive index of the solution, F is two-photon excited fluorescence integral intensity and Φ is the fluorescence quantum yield.

Wide-Field Fluorescence Microscopy Imaging and Two-Photon Fluorescence Microscopy Imaging of SiHa Cells Stained with 9B-HVC

SiHa cells were cultured in Dulbecco's modified Eagle's medium (DMEM) supplemented with penicillin/streptomycin and 10% bovine calf serum with 5% CO_2 at 37 °C. The 9B-HVC were dissolved in DMSO at a concentration of 1 mM and subsequently diluted in DMEM medium for using. Cultured cells grown on glass coverslips were incubated with 9B-HVC and/or MitoTracker Orange (MTO, Invitrogen) in a 5% CO_2 incubator at 37 °C and then imaged with WFM and TPM.

WFM images were acquired with an Olympus IX71 inverted microscope coupling with a CCD and a DP

Table 1 Photophysical properties of the compounds in different environment

Compound	H_2O			MeCN			Gly		
	λ_1/λ_2 [nm]	ε [$M^{-1}\cdot cm^{-1}$]	Φ [%]	λ_1/λ_2 [nm]	ε [$M^{-1}\cdot cm^{-1}$]	Φ [%]	λ_1/λ_2 [nm]	ε [$M^{-1}\cdot cm^{-1}$]	Φ [%]
MVC	411/561	2.70×10^4	0.31	418/561	2.64×10^4	6.47	429/552	2.40×10^4	19.08
HVC	415/564	3.18×10^4	0.31	421/558	2.84×10^4	6.69	431/553	2.82×10^4	15.63
9B-MVC	420/568	2.78×10^4	0.48	431/570	3.70×10^4	7.45	438/562	3.26×10^4	21.68
9B-HVC	427/570	3.04×10^4	0.39	434/570	3.04×10^4	9.66	443/563	2.78×10^4	25.30

λ_1 and λ_2 are linear absorption, single- photon fluorescent maximum peak, respectively; ε is molar absorptivity; Φ is single-photon fluorescence quantum yield determined using coumarin 307 (Φ=0.56) [36] as the standard

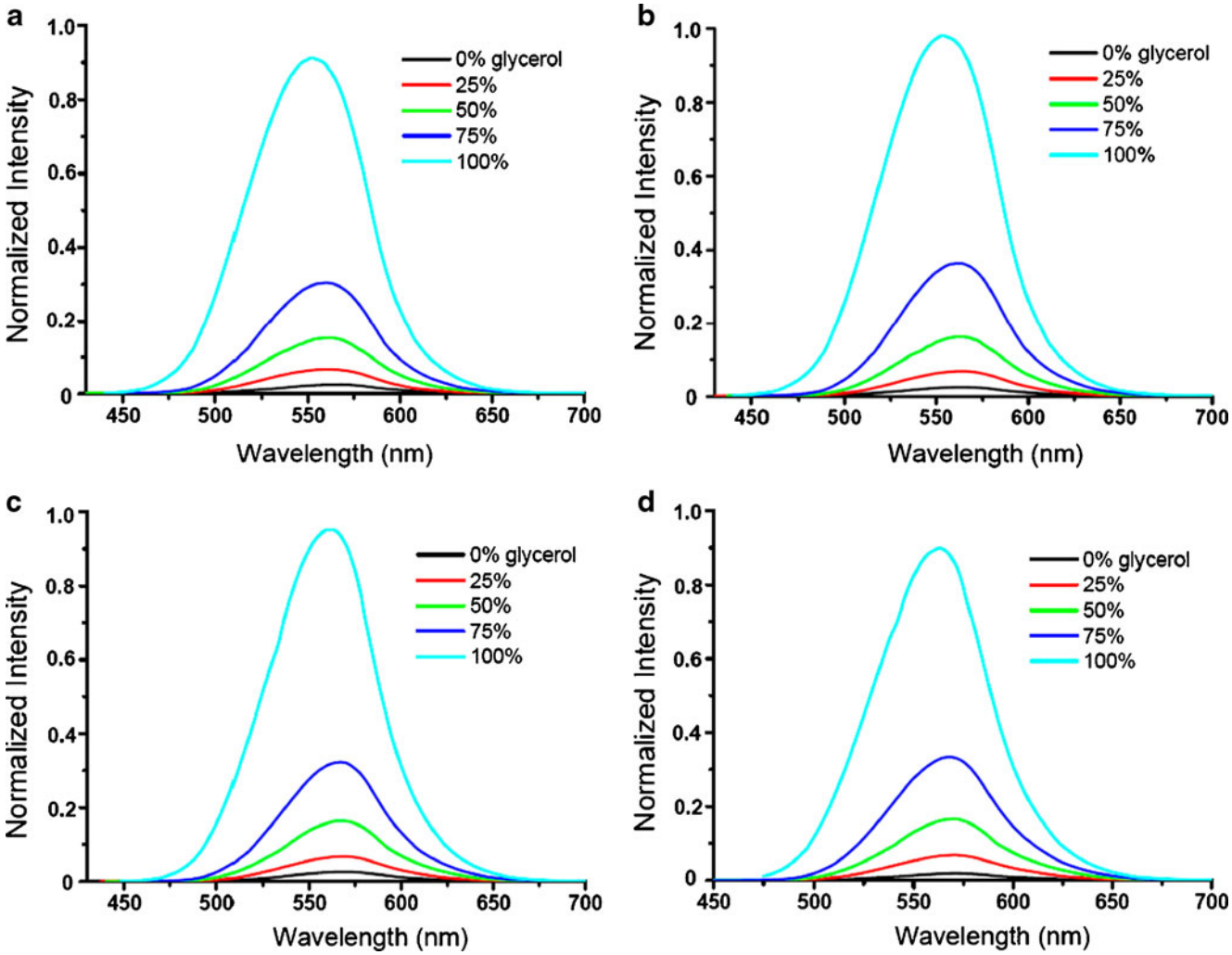

Fig. 2 Single-photon excited fluorescence spectra of compounds in glycerol/water mixtures at room temperature: **a** MVC, **b** HVC, **c** 9B-MVC, **d** 9B-HVC. Concentration: 5.0×10^{-6} M

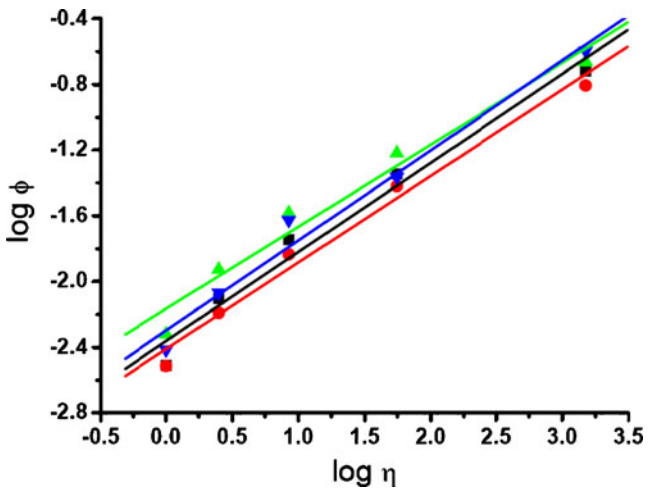

Fig. 3 The plots of the log(ϕ) versus log(η) of these compounds in glycerol/water mixtures. *Black*: MVC, *Red*: HVC, *Green*: 9B-MVC and *Blue*: 9B-HVC

controller software. The fluorescence of 9B-HVC and MTO were excited and collected through U-MNIBA3 and U-MWG2, respectively.

All of TPM microscopic photos were obtained with Olympus FV 300 Laser Confocal System with a 60× water objective (N.A.=1.25) and photomultiplier tubes. A Ti: sapphire laser (Coherent) was used to excite specimen at 800 nm. The total power provided by laser source can maintain stable and the incident power on samples was modified by means of an attenuator and examined with Power Monitor (Coherent). Fluorescence of 9B-HVC was collected with a beam splitter DM570 and BA510-540 nm bandpass emission filter combination. The differential interference contrast (DIC) image was taken with 488 nm Arion laser.

Cell-Viability Assay

The study of the effect of 9B-HVC on viability of cells was carried out using the methylthiazolyldiphenyl-tetrazolium

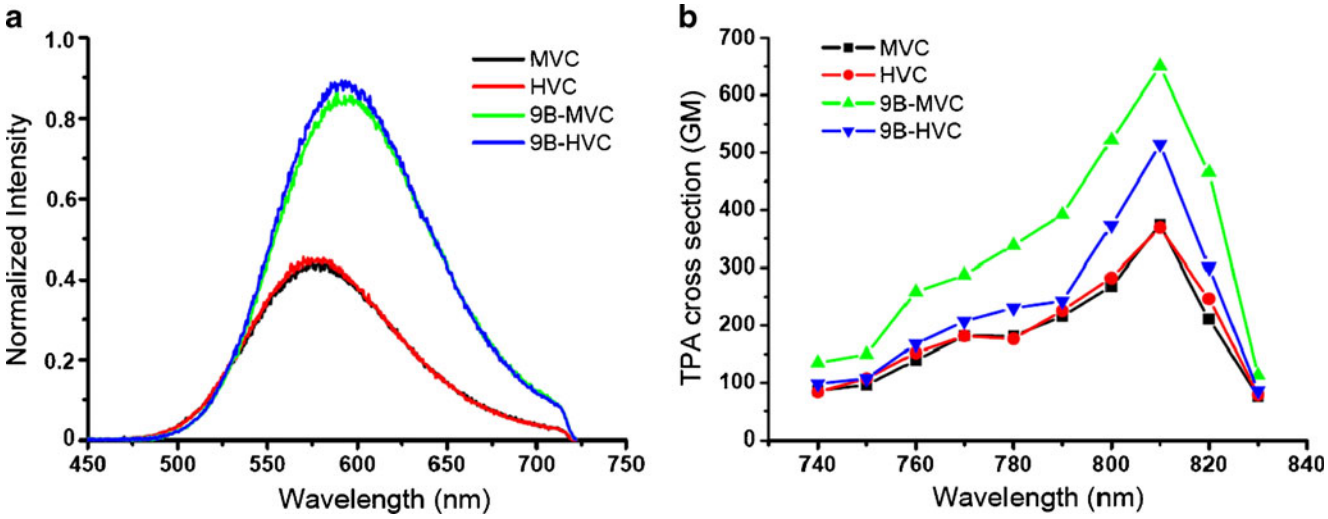

Fig. 4 **a** Two-photon excited fluorescence spectra of four compounds in MeCN at the optimal excitation wavelength of 810 nm. **b** Two-photon absorption cross sections of four compounds in MeCN versus excitation wavelengths. All concentration: 1×10^{-4} M. The experimental uncertainty in the cross-sections values is 15%

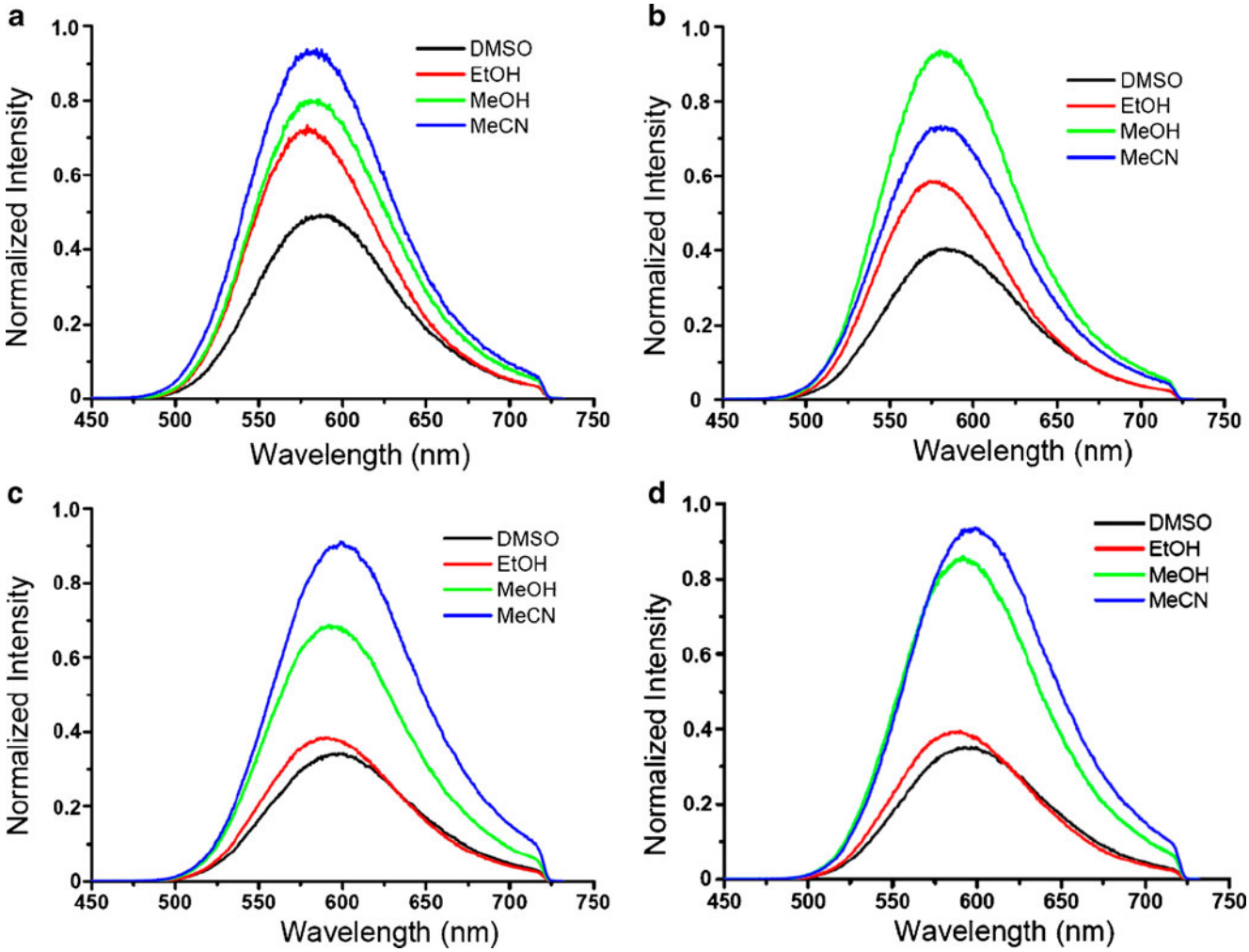

Fig. 5 Two-photon excited fluorescence spectra of compounds in four polar solvents: **a** MVC, **b** HVC, **c** 9B-MVC, **d** 9B-HVC. Excitation wavelength: 800 nm. All concentration: 1×10^{-4} M

Table 2 TPE maximum emission and TPA cross section values of compounds in various solvents

Solvent	MVC		HVC		9B-MVC		9B-HVC	
	λ [nm]	δ [GM]	λ [nm]	δ [GM]	λ [nm]	δ [GM]	λ [nm]	δ [GM]
MeCN	585	268	580	283	599	522	600	373
MeOH	585	309	580	239	593	326	594	333
EtOH	579	135	583	112	590	160	590	108
DMSO	587	99	580	101	598	120	597	79

λ is two-photon fluorescent maximum peak; δ is two-photon absorption cross sections determined using coumarin 307 (δ=27.7 GM) [34] at 800 nm; 1GM=10^{-50} $cm^4 \cdot s \cdot photon^{-1}$; Concentration of samples for δ: 100 μM; error limit: 15%

bromide (MTT) assay [35]. SiHa cell cultures were grown in 96-well plates (ca. 1×10^4 cells/well) in DMEM containing 10% bovine calf serum in a 5% CO_2 incubator at 37 °C. For examining the short-term cytotoxic effect, cells were then incubated with 9B-HVC at 2 μM for 24, 48 and 72 h, then MTT assay was used as described. Non-treated cells were used as control. Each individual cytotoxic experiment was repeated for three times.

Results and Disscussion

Linear Absorption and Single-Photon Excited Fluorescence of Compounds

The UV-vis absorption (a) and one-photon fluorescence (b) spectra of compounds in MeCN are shown in Fig. 1 and the relevant photophysical properties of these compounds are summarized in Table 1. These compounds exhibit the maximum absorption at 418 nm - 434 nm and have large ε_{max} of 2.64×10^4 $M^{-1}\cdot$ cm^{-1}–3.70×10^4 $M^{-1}\cdot$ cm^{-1} in MeCN. From Fig. 1b, one can observe that 9B-HVC/9B-MVC emit the stronger fluorescence than HVC/MVC and the emission maximum of these compounds are at 561–570 nm in MeCN. The higher fluorescent intensity of 9B-HVC/9B-MVC might be attributed to the substitution of the *n*-butyl for H in carbazole moiety which possesses the electron-donating ability. It is well known that an intramolecular charge transfer (ICT) state can be formed between the electron–acceptor and the electron–donor in carbazole derivatives [37, 38]. In order to further elucidate whether the ICT character is predominant in the photophysical behavior of these compounds, the one-photon fluorescent spectra of compounds in glycerol/water mixture, which is often used to clarify the ICT character of fluorophores [39], were recorded. The results show that when increasing glycerol content, the fluorescent intensity distinctly enhances (Fig. 2). And the plots (Fig. 3) of log Φ of compounds versus the log η, where η is viscosity of each glycerol/water mixture obtained from the Handbook [40], show linear relationship [39]. Thus we suggest that in these compounds, the larger dipole moment in the excited state contributed by the intensive ICT interacts strongly with the water, which could lead to intramolecular twist of the vinyl group resulting in nonradiative decay by forming twisting intramolecular charge transfer (TICT) state. However, with the decrease of the polarity ($\varepsilon_{glycerol}$=37, ε_{water}=81.2) and increase of the viscosity ($\eta_{glycerol}$=1,499, η_{water}=1.005) of solvents, the molecular torsional motions of the vinyl groups would be restricted, consequently the fluorescence emission of compounds restores. Carefully observing Table 1, these compounds have lowest Φ in water, but they can fluoresce in non-water environment such as MeCN, furthermore the Φ of all four compounds in viscous non-water environment such as glycerol is highest in the three environments, which also shows the influence of the environments on fluorescence of compounds due to the predominant actions of ICT character. Thus, if these

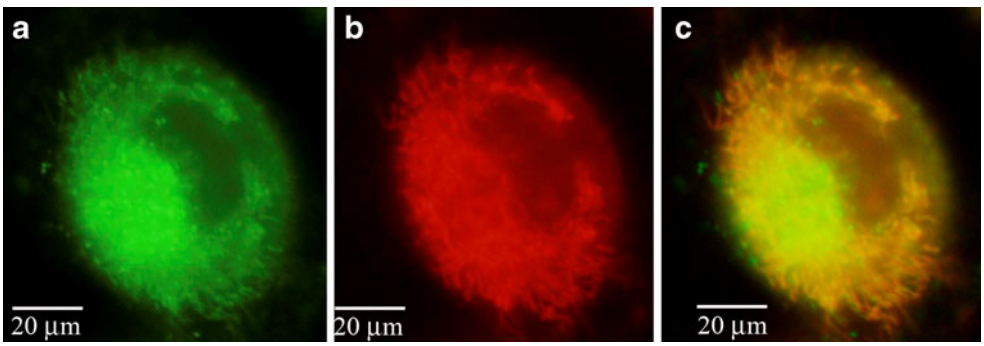

Fig. 6 Wide-field fluorescence images of SiHa cancer cells incubated with 9B-HVC (2 μM) for overnight and with MTO (25 nM) for 30 min. **a** Fluorescence of 9B-HVC, **b** fluorescence of MTO, and **c** the merged picture

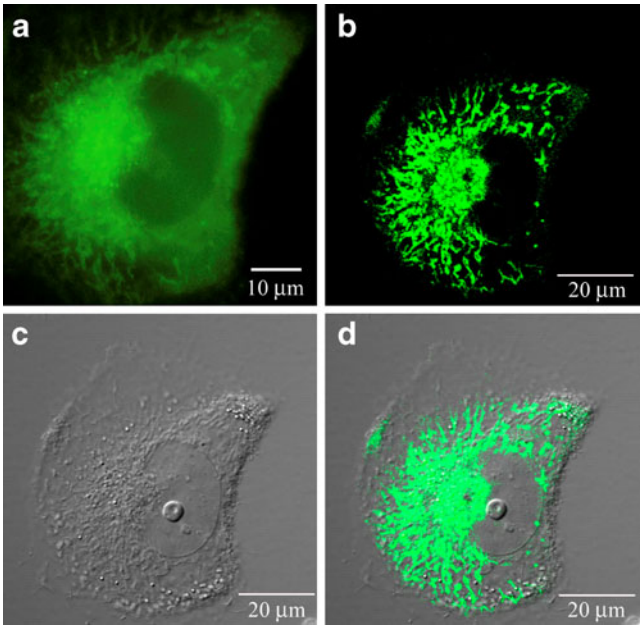

Fig. 7 Images of SiHa cells incubated with 2 μM 9B-HVC for overnight. **a** WFM image, **b** TPM image, **c** DIC image, **d** merge image of **b** and **c**

cationics can exclusively accumulate in mitochondria, they can possess the added advantage that it is essentially nonfluorescence in aqueous solutions and only becomes fluorescent once it accumulates in the lipid environment of mitochondria. Hence, their background fluorescence is low even negligible, which enables researchers to clearly visualize mitochondria in living cell.

Two-Photon Excited Fluorescence of Compounds

As shown in Fig. 4a, these compounds presented a bright two-photon excited fluorescence centered at 573–591 nm in MeCN with an optimal excitation wavelength of 810 nm and 9B-MVC/9B-HVC exhibit higher TPF than that of MVC/HVC which was similar with the photophysical behavior by one-photon excitation. In order to investigate the influence of excited wavelengths on δ_{TPA}, the laser was tuned from 740 nm to 830 nm, and the two-photon absorption spectra of these compounds were shown in Fig. 4b. The maximum δ_{TPA} of these compounds occur at a wavelength of 810 nm and their highest δ_{TPA} values are calculated to be 268 GM (MVC), 283 GM (HVC), 522 GM (9B-MVC) and 373 GM (9B-HVC) in MeCN, respectively. Furthermore, the two-photon excited fluorescence spectra of compounds in four common solvents were measured at a wavelength of 800 nm which is an optimal excitation wavelength provided by commercial mode-locked Ti: sapphire laser source (Fig. 5) and the corresponding δ_{TPA} are listed in Table 2. From Fig. 5, one can see that all spectra have maximum emission longer than 570 nm, which benefiting visualization of living specimen, at the same time the two-photon excited fluorescence of compounds exhibit evident solvatochromism due to their ICT character [41, 42]. It is worth underlining that these four compounds exhibit large δ_{TPA} in all solvents and are more than 1 or 2 order of magnitude larger than that of many commercial fluorophores widely used in biology, such as fluorescein (38 GM), Indo-1 (4.5 GM), and EB (7 GM) [26, 43].

Visualization of Mitochondria Stained with 9B-HVC in WFM and TPM

To demonstrate the potentiality of 9B-HVC with larger δ_{TPA} for imaging mitochondria in living cells, a standard double-staining experiment with 9B-HVC and MTO (a commercial mitochondria probe) has been carried out. The SiHa cells were firstly incubated with 9B-HVC at 2 μM overnight in a 5% CO_2 incubator at 37 °C and then stained with 25 nM MTO. Subsequently, the cells were washed to remove the excess of unbound probe and imaged by WFM immediately. As shown in Fig. 6, the fluorescent picture of 9B-HVC (Fig. 6a) is wholly consistent with that of MTO (Fig. 6b), and the substantial overlap between 9B-HVC and MTO in the merged image (Fig. 6c) emits orange fluorescence. According to Fig 6, the position, shape and amounts of the mitochondria labeled by 9B-HVC are the same as that of MTO. These results can confirm that 9B-HVC is a potential fluorescent mitochondria probe. To further examine the ability of 9B-HVC for imaging living cell on TPM, the same cell stained by 9B-HVC was imaged with WFM, DIC and TPM simultaneously (Fig.7). Figure 7a was obtained with WFM and Fig. 7b was acquired by TPM using a 5 mW of beam at 800 nm, 200 fs pulses and 76 MHz (the power is safe for living specimen) [16]. The DIC image (Fig. 7c) of cell was taken with 488 nm Arion laser immediately prior to the TPM imaging and Fig. 7d presented the merged picture of Fig. 7b and c. Compared with Fig. 7a, b show preferable contrast with high brightness and Fig. 7d gives the clear distribution of mitochondria, which can better overlay that from DIC picture. Altogether these results demonstrate that 9B-HVC can exclusively target to mitochondria and be applicable to TPM imaging.

Table 3 Cytotoxicity Data (SiHa, 2 μM)[a]

incubate time	24 h	48 h	72 h
% cell survival	99±3	86±3	71±7

[a] Cell viability was quantified by the MTT assay (mean±SD)

Short-Term Cytotoxicity of 9B-HVC

Cytotoxicity of 9B-HVC was evaluated in SiHa cells by MTT assay. The cell viability assay data of SiHa cells treated with 2 μM 9B-HVC during different incubation time was quantified (Table 3). The results show that SiHa cells show nearly 100% viability for 24 h, and longer incubating time can result in decreased cell survival, 86% for 48 h and 71% for 72 h. Thus the concentrations at a micromolar order of magnitude and short treating time for 9B-HVC could be considered as nontoxic.

Conclusion

We have developed a series of two-photon fluorescent compounds based on donor- Π—acceptor (D-Π-A) structure derived from carbazole. These compounds exhibit TPF features and have larger δ_{TPA} than that of the conventional fluorescent probes. The further study demonstrates that 9B-HVC possesses significant potential for imaging mitochondria in TPM with better specificity for mitochondria localization and without apparent cytotoxic effects at micromolar concentration. The results reported in this paper provide a useful design and synthesis strategy for the two-photon fluorescent probes of mitochondria.

Acknowledgement For financial support, we thank the National Science Foundation of China (50673053, 50173015, 50925205, 50990303 and 50872070) and NSFC/RGC (50218001). Also Open Project of State Key Laboratory of Supramolecular Structure and Materials, Independent Innovation Foundation of Shandong University, (2009JC011) and the Program of Introducing Talents of Discipline to Universities in China (111 programNo. b06015).

References

1. Sanadi DR (1965) Energy-linked reactions in mitochondria. Annu Rev Biochem 34:21–48
2. Petit PX, Susin SA, Zamzami N, Mignotte B, Kroemer G (1996) Mitochondria and programmed cell death: back to the future. FEBS Lett 396(1):7–13
3. Lambert AJ, Brand MD (2009) Reactive oxygen species production by mitochondria. Methods Mol Biol 554:165–181
4. Nicholls DG (2005) Mitochondria and calcium signaling. Cell Calcium 38(3-4):311–317
5. Boldogh IR, Pon LA (2007) Mitochondria on the move. Trends Cell Biol 17(10):502–510
6. Rouiller C (1960) Physiological and pathological changes in mitochondrial morphology. Int Rev Cytol 9:227–292
7. Hakenbrock CR (1968) Ultrastructural bases for metabolically linked mechanical activity in mitochondria:II.electron transport-linked ultrastructural transformations in mitochondria. J Cell Biol 37(2):345–369
8. Johnson LV, Summerhayes IC, Chen LB (1982) Decreased uptake and retention of rhodamine 123 by mitochondria in a feline sarcoma virus-transformed mink cells. Cell 28(1):7–14
9. Kahlert S, Zündorf G, Reiser G (2008) Detection of de- and hyperpolarization of mitochondria of cultured astrocytes and neurons by the cationic fluorescent dye rhodamine 123. J Neurosci Methods 171(1):87–92
10. So PTC, Dong CY, Masters BR, Berland KM (2000) Two-photon excitation fluorescence microscopy. Annu Rev Biomed Eng 2:399–429
11. Rubart M (2004) Two-photon microscopy of cells and tissue. Circ Res 95(12):1154–1166
12. Wang BG, König K, Halbhuber KJ (2010) Two-photon microscopy of deep intravital tissues and its merits in clinical research. J Microsc 238(1):1–20
13. Yuan T, Gao SS, Saggau P, Oghalai JS (2010) Calcium imaging of inner ear hair cells within the cochlear epithelium of mice using two-photon microscopy. J Biomed Opt 15(1):016002
14. Merlo F, Balduzzi R, Cupello A, Robello M (2004) Immunocytochemical study by two photon fluorescence microscopy of the distribution of GABA(A) receptor subunits in rat cerebellar granule cells in culture. Amino Acids 26(1):77–84
15. Ghosh S, Kim D, So P, Blankschtein D (2008) Visualization and quantification of skin barrier perturbation induced by surfactant-humectant systems using two-photon fluorescence microscopy. J Cosmet Sci 59(4):263–89
16. Koepsell H (2007) In vivo two-photon fluorescence microscopy opens a new area for investigation of the excretion of cationic drugs in the kidney. Kidney Int 72(4):387–388
17. Dedov VN, Cox GC, Roufogalis BD (2001) Visualisation of mitochondria in living neurons with single- and two-photon fluorescence laser microscopy. Micron 32(7):653–660
18. Mqller M, Mironov SL, Ivannikov MV, Schmidt J, Richter DW (2005) Mitochondrial organization and motility probed by two-photon microscopy in cultured mouse brainstem neurons. Exp Cell Res 303(1):114–127
19. Feijó JA, Cox G (2001) Visualization of meiotic events in intact living anthers by means of two-photon microscopy. Micron 32 (7):679–684
20. Chen TS, Zeng SQ, Luo QM, Zhang ZH, Zhou W (2002) High-order photobleaching of green fluorescent proteininside live cells in two-photon excitation microscopy. Biochem Biophys Res Commun 291(5):1272–1275
21. Patterson GH, Piston DW (2000) Photobleaching in two-photon excitation microscopy. Biophys J 78(4):2159–2162
22. Kim HM, Cho BR (2009) Two-photon probes for intracellular free metal ions, acidic aesicles, and lipid rafts in live tissues. Acc Chem Res 42(7):863–872
23. Lim CS, Kang DW, Tian YS, Han JH, Hwang HL, Cho BR (2010) Detection of mercury in fish organs with a two-photon fluorescent probe. Chem Commun 46(14):2388–2390
24. Lee JH, Lim CS, Tian YS, Han JH, Cho BR (2010) A two-photon fluorescent probe for thiols in live cells and tissues. J Am Chem Soc 132(4):1216–1217
25. Morales AR, Schafer-Hales KJ, Yanez CO, Bondar MV, Przhonska OV, Marcus AI, Belfield KD (2009) Excited state intramolecular proton transfer and photophysics of a new fluorenyl two-photon fluorescent probe. Chemphyschem 10(12):2073–2081
26. Fantin VR, Berardi MJ, Scorrano L, Korsmeyer SJ, Leder P (2002) A novel mitochondriotoxic small molecule that selectively inhibits tumor cell growth. Cancer Cell 2(1):29–42
27. Filomeni G, Piccirillo S, Graziani I, Cardaci S, Da Costa Ferreira AM, Rotilio G, Ciriolo MR (2009) The isatin-schiff base copper (II) complex $Cu(isaepy)_2$ acts as delocalized lipophilic cation, yields widespread mitochondrial oxidative damage and induces AMP-activated protein kinase-dependent apoptosis. Carcinogenesis 30(7):1115–1124
28. Johnson LV, WalshML CLB (1980) Localization of mitochondria in living cells with rhodamine 123. Proc Natl Acad Sci USA 77 (2):990–994

29. Murphy MP (2008) Targeting lipophilic cations to mitochondria. Biochim Biophys Acta 1777(7–8):1028–1031
30. Ross MF, Kelso GF, Blaikie FH, James AM, Cochemé HM, Filipovska A, Da Ros T, Hurd T, Smith RA, Murphy MP (2005) Lipophilic triphenylphosphonium cations as tools in mitochondrial bioenergetics and free radical biology. Biochemistry (Moscow) 70 (2):222–230
31. Hoegl H (1965) On photoelectric effects in polymers and their sensitization by dopants. J Phys Chem 69(3):755–766
32. Coe BJ (2006) Switchable nonlinear optical metallochromophores with pyridinium electron acceptor groups. Acc Chem Res 39 (6):383–393
33. Zhang X, Yu XQ, Sun YM, Xu HY, Feng YG, Huang BB, Tao XT, Jiang MH (2006) Synthesis, structure and nonlinear optical properties of two new one and two-branch two-photon polymerization initiators. Chem Phys 328(1–3):103–110
34. Xu C, Webb WW (1996) Measurement of two-photon excitation cross sections of molecular fluorophores with data from 690 to 1050 nm. J Opt Soc Am B 13(3):481–491
35. Edmondson JM, Armstrong LS, Martinez AO (1988) A rapid and simple MTT-based spectrophotometric assay for determining drug sensitivity in monolayer cultures. J Tissue Cult Methods 11 (1):15–17
36. Lee S, Thomas KR, Thayumanavan S, Bardeen CJ (2005) Dependence of the two-photon absorption cross section on the conjugation of the phenylacetylene linker in dipolar donor-bridge-acceptor chromophores. J Phys Chem A 109(43):9767–9774
37. Castex MC, Olivero C, Pichler G, Adés D, Cloutet E, Siove A (2001) Photoluminescence of donor–acceptor carbazole chromophores. Synth Met 122(1):59–61
38. Adés D, Boucard V, Cloutet E, Siove A, Olivero C, Castex MC, Pichler G (2000) Photoluminescence of donor-acceptor carbazole-based molecules in amorphous and powder forms. J Appl Phys 87 (10):7290–7293
39. Chang CC, Chu JF, Kuo HH, Kang CC, Lin SH, Chang TC (2006) Solvent effect on photophysical properties of a fluorescence probe: BMVC. J Lumin 119:84–90
40. Dean JA (ed) (1973) Handbook of chemistry. McGraw-Hill, New York
41. Bosch P, FernaÂndez-Arizpe A, Mateo JL, Lozano AE, Noheda P (2000) New fluorescent probes for monitoring polymerisation reactions: 1. Synthesis, solvatochromism and emission properties. J Photochem Photobiol A Chem 133(1–2):51–57
42. Qin W, Baruah M, Sliwa M, Van der Auweraer M, De Borggraeve WM, Beljonne D, Van Averbeke B, Boens N (2008) Ratiometric, fluorescent BODIPY dye with aza crown ether functionality: synthesis, solvatochromism, and metal ion complex formation. J Phys Chem A 112(27):6104–6114
43. Malak H, Castellano FN, Gryczynski I, Lakowicz JR (1997) Two-photon excitation of ethidium bromide labeled DNA. Biophys Chem 67:35–41